



# Coevolution of host–plasmid pairs facilitates the emergence of novel multidrug resistance

Hannah Jordt<sup>1,2</sup>, Thibault Stalder<sup>2,3</sup>, Olivia Kosterlitz<sup>1,2</sup>, José M. Ponciano<sup>4</sup>, Eva M. Top<sup>1,2,3</sup>✉ and Benjamin Kerr<sup>1,2</sup>✉

**Multidrug resistance (MDR) of pathogens is an ongoing public health crisis exacerbated by the horizontal transfer of antibiotic resistance genes via conjugative plasmids. Factors that stabilize these plasmids in bacterial communities contribute to an even higher incidence of MDR, given the increased likelihood that a host will already contain a plasmid when it acquires another through conjugation. Here, we show one such stabilizing factor is host–plasmid coevolution under antibiotic selection, which facilitated the emergence of MDR via two distinct plasmids in communities consisting of *Escherichia coli* and *Klebsiella pneumoniae* once antibiotics were removed. In our system, evolution promoted greater stability of a plasmid in its coevolved host. Further, pleiotropic effects resulted in greater plasmid persistence in both novel host–plasmid combinations and, in some cases, multi-plasmid hosts. This evolved stability favoured the generation of MDR cells and thwarted their loss within communities with multiple plasmids. By selecting for plasmid persistence, the application of antibiotics may promote MDR well after their original period of use.**

Plasmids are found in bacteria as extrachromosomal pieces of DNA that replicate separately from the host chromosome. They are a common repository of genes encoding antibiotic resistance, and conjugative plasmids can facilitate the spread of such genes via horizontal transfer<sup>1</sup>. The acquisition of a new plasmid can be costly for its host due to the burden imposed by plasmid-related processes such as replication, conjugation and gene expression or the ‘interference’ associated with interactions between plasmid-encoded proteins and cell housekeeping functions<sup>2–4</sup>. In the presence of an antibiotic, these costs can be outweighed by the benefit of plasmid-encoded resistance. In its absence, however, the costs are predicted to give a competitive advantage to plasmid-free cells. If plasmid loss occurs due to improper segregation of the plasmid during cell division (segregational loss), such costs could lead to a selective decrease in the fraction of plasmid-bearing cells in the population. In this light, it is puzzling that plasmids encoding antibiotic resistance often show high persistence<sup>5</sup>, here defined as the capacity of a population, wherein all cells initially contain the plasmid, to maintain a high fraction of plasmid-bearing cells over time in the absence of drugs.

Solutions to this ‘plasmid paradox’<sup>6</sup> involve processes that counterbalance, disrupt or diminish selection against the plasmid. For instance, high rates of plasmid conjugation can transform plasmid-free cells into plasmid-containing cells, thereby counterbalancing selection for segregants and contributing to plasmid persistence<sup>7,8</sup>. Low rates of segregational loss or the incorporation of a post-segregational killing mechanism that inhibits growth of plasmid-free cells can disrupt selection against the plasmid; these mechanisms contribute to plasmid persistence by ensuring a dearth of (fitter) plasmid-free competitors<sup>9,10</sup>. Finally, compensatory mutations occurring in the host chromosome or the plasmid during coevolution can alleviate plasmid costs, which diminishes the strength of selection against the plasmid<sup>11–21</sup>.

Mutations that enhance conjugation, diminish segregational loss or relieve the fitness cost of plasmids encoding antibiotic resistance allow the plasmids to better persist in the absence of drugs. These mutations could improve persistence strictly within the original coevolutionary context or additionally in novel host–plasmid combinations. Either way, these mutants serve as a stable source that can spread resistance to new strains and species within the microbial community. If recipient hosts are already resistant to a different antibiotic, novel multidrug resistance (MDR) results. Therefore, in bacterial communities where prior evolution led to greater persistence of conjugative plasmids encoding resistance to different antibiotics, we expect the likelihood of hosts acquiring multiple distinct plasmids to be higher, thereby priming the emergence of MDR.

Antibiotic usage is on the rise, resulting in higher incidences of resistance in species of high clinical importance within the family Enterobacteriaceae<sup>22–24</sup>. This resistance is often caused by multiple self-transmissible plasmids, even leading to extended-resistant *E. coli* and pan-resistant *K. pneumoniae*<sup>25,26</sup>. Indeed, evolution of MDR in *K. pneumoniae* is mainly driven by the acquisition of multiple resistance plasmids<sup>27</sup>, which was reported to be particularly the case in clones found in clinical outbreaks<sup>28,29</sup>. It is thus critical to explore the effects of evolution under antibiotic selection on the subsequent likelihood of emergence of novel MDR via horizontally transmitted resistance genes in Enterobacteriaceae communities.

## Predicted effects of coevolution

To explore how plasmid dynamics affect the emergence of MDR in bacterial communities, we consider a system involving two bacterial species and two conjugative plasmids, each encoding resistance to a different antibiotic. For simplicity, in this example, we focus on the cost of plasmid carriage as the determinant of plasmid persistence. However, we note that the rate of plasmid conjugation or segregational loss could also be contributing factors. For any host–plasmid pair in this example, we predict that the plasmid-associated

<sup>1</sup>Biology Department, University of Washington, Seattle, WA, USA. <sup>2</sup>BEACON Center for the Study of Evolution in Action, East Lansing, MI, USA.

<sup>3</sup>Department of Biological Sciences and Institute for Bioinformatics and Evolutionary Studies, University of Idaho, Moscow, ID, USA. <sup>4</sup>Department of Biology, University of Florida, Gainesville, FL, USA. ✉e-mail: [evatop@uidaho.edu](mailto:evatop@uidaho.edu); [kerrb@uw.edu](mailto:kerrb@uw.edu)

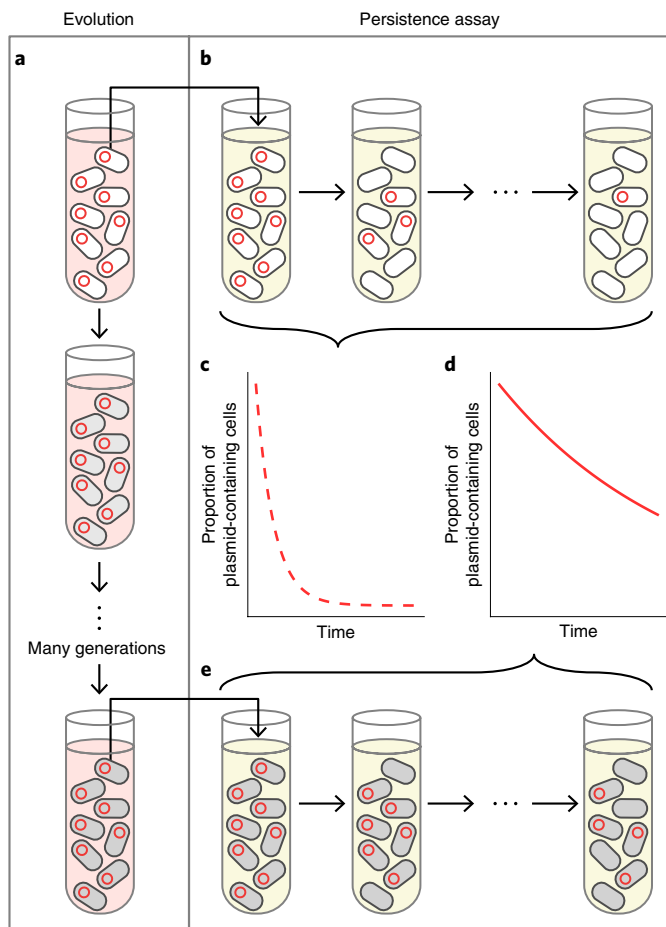


**Fig. 1 | Predictions of the effects of host-plasmid coevolution on plasmid persistence.** **a**, A hypothetical population of bacteria evolving for many generations (represented as a culture propagated via serial batch transfer) in the presence of an antibiotic (red-shaded medium) selecting for maintenance of a plasmid (red circle) encoding resistance. Evolutionary changes are represented by progressively darker grey shading of the bacteria over the sequence. **b**, An isolate from the ancestral population is grown and propagated without the antibiotic (yellow-shaded medium) over a small number of transfers. **c**, When the plasmid is costly, we predict the proportion of plasmid-containing cells decreases rapidly as they are outcompeted by plasmid-free cells generated via segregational loss (dashed line). **d,e**, If evolutionary changes include mutations that compensate for the cost of plasmid carriage, we predict the proportional loss of plasmid-containing cells is slower (solid line; **d**), as would occur when an isolate from the evolved population with compensatory mutations is grown and propagated without the antibiotic (**e**).

cost will affect the rate of plasmid loss from a population of hosts propagated in the absence of antibiotics. If the magnitude of the cost is high, de novo segregants will displace plasmid-bearing cells quickly (Fig. 1b), producing a steep plasmid decay curve (Fig. 1c). Yet evolution in the presence of the relevant antibiotic (Fig. 1a) may lead to a reduction in the cost, which would then result in greater plasmid persistence (Fig. 1d,e). Such predictions are consistent with the results from previous studies<sup>10–13</sup>. By incorporating a second host–plasmid pair, we expand upon these prior studies by exploring the emergence of MDR under drug-free conditions when the two evolved bacterial species, each harbouring a distinct plasmid, are now mixed. We predict that if plasmid persistence is low, the incidence of MDR will be low (Fig. 2b,c). However, if each bacterial species first coevolved with a distinct plasmid separately before coming

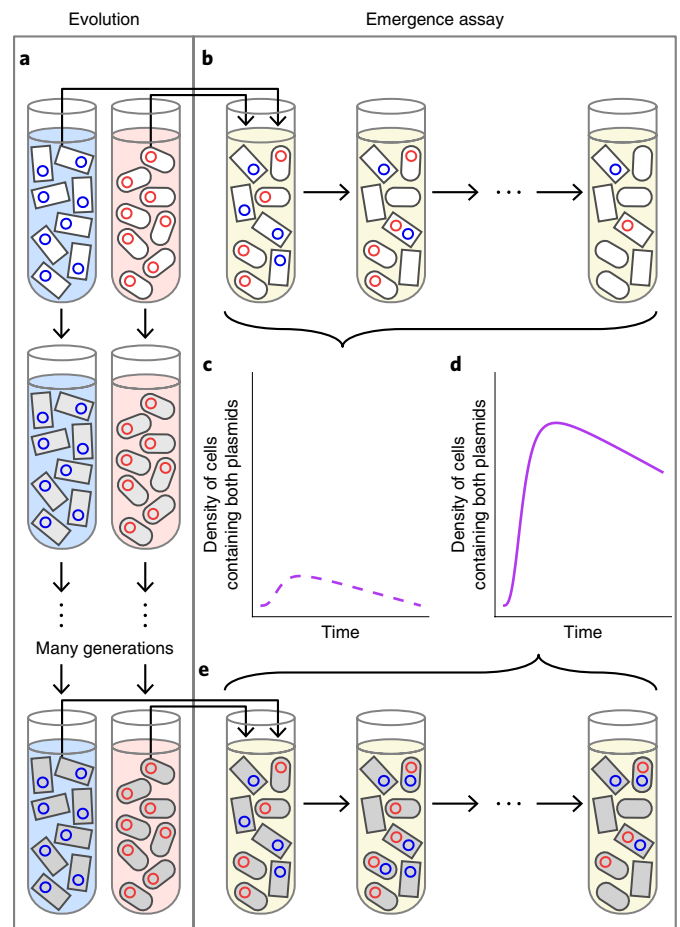


**Fig. 2 | Predictions of the effects of host-plasmid coevolution on MDR emergence.** **a**, Two different species of bacteria are considered. Cells of the first species are represented as rectangles, while cells of the second are given as rods. Cells from each species possess a distinct plasmid represented by the different coloured circles. Both species evolve independently for many generations in the presence of an antibiotic that selects for maintenance of the plasmid (blue-shaded medium selects for blue plasmid and red-shaded medium selects for red plasmid). **b**, Isolates from each ancestral population are mixed in medium without antibiotics and tracked over a small number of transfers. **c**, In the case of **b**, we predict low numbers of MDR cells (containing both plasmids) arising (dashed line). **d,e**, However, we predict the incidence of MDR cells is higher (solid line; **d**), when isolates from the evolved populations are mixed in antibiotic-free medium (**e**).

together as a community (Fig. 2a), the incidence of MDR would be higher (Fig. 2d,e). Once a cell harbours both plasmids, MDR could be maintained either due to maintenance of both plasmids or by the incorporation of the resistance genes into the chromosome or a single maintained plasmid. Regardless, we assume that by creating more stable sources of plasmids, the opportunities for conjugation between host types increase once they are in a mixed community, contributing to an increase in novel MDR. A more rigorous treatment of these topics via a mathematical model supports these predictions (see Supplementary Information, section 1, and Extended Data Figs. 1 and 2).

## Results

**Evolution increases plasmid persistence.** To empirically test our predictions, we introduced conjugative plasmid pALTS28 (hereafter ‘p1’) encoding tetracycline resistance into an *E. coli* host

(hereafter 'E') and conjugative plasmid pALTS29 (hereafter 'p2') encoding chloramphenicol resistance into a *K. pneumoniae* host (hereafter 'K'). We denote these strains as E(p1) and K(p2), where the host species is listed first and the plasmid inside the host is given in parentheses. Plasmid-free cells are indicated by E( $\emptyset$ ) and K( $\emptyset$ ) and cells that contain both plasmids are denoted E(p1,p2) and K(p1,p2). As shown in Fig. 2a, each plasmid-bearing host was propagated in the presence of the relevant antibiotic for about 400 generations. To signify that evolution has taken place, and to convey information about the context of evolution, we add subscripts to both the host and the plasmid. Thus,  $E_1(p1_E)$  is an *E. coli* cell from a bacterial lineage that evolved with plasmid p1 currently possessing plasmid p1 from a plasmid lineage that evolved in *E. coli*. The reason for the complex notation is that mutations may occur in either the host chromosome or the plasmid<sup>17,30</sup> and that we need to specify the evolutionary histories of both hosts and plasmids and indicate new plasmid–host combinations generated by conjugation. For instance,  $K_2(p1_E, p2_K)$  is a *K. pneumoniae* cell with a coevolutionary history with plasmid p2, which currently contains both this coevolved plasmid p2 and plasmid p1 that evolved in the *E. coli* host.

Both plasmids were unstable in the absence of antibiotics before coevolving with their hosts: p1 was rapidly lost from *E. coli* (Fig. 3a) and p2 from *K. pneumoniae* (Fig. 3c). That is, separate populations of E(p1) and K(p2) were rapidly overtaken by E( $\emptyset$ ) and K( $\emptyset$ ) cells, respectively. However, after evolution, plasmids p1 and p2 each persisted to a greater degree in their respective coevolved hosts across all replicates (Fig. 3b,d). Statistical support for these differences was obtained using a plasmid population dynamic model previously described<sup>31–33</sup> to fit and compare plasmid persistence curves (see Methods and Supplementary Information, section IV). All aspects of this protocol were also completed for the other plasmid–host combinations, E(p2) and K(p1), and nearly all evolved lines exhibited a similar increase in persistence compared to their ancestors (Extended Data Fig. 3).

**Evolution increases emergence of MDR.** We then asked how plasmid–host coevolution would affect the emergence of novel MDR in a mixed-species culture. As diagrammed in Fig. 2b,e, we cocultured three replicates of the ancestral species E(p1) with K(p2), and three replicates of the evolved species  $E_1(p1_E)$  with  $K_2(p2_K)$ , in serial batch culture in the absence of antibiotics. Note that the evolved isolates used were those that correspond to the persistence profiles indicated by the star symbols in Fig. 3. Using selective plating to track the eight potential cell types that could arise in such a coculture, we found a higher cumulative incidence of *K. pneumoniae* cells containing both plasmids in the evolved assemblage (two-tailed Welch's *t*-test,  $t = -7.904$ , 95% confidence interval (CI) =  $[-11199698, -3304356]$ , d.f. = 2,  $P = 0.0156$ ,  $\alpha = 0.025$  after a Bonferroni correction for two comparisons (*E. coli* and *K. pneumoniae*; Supplementary Information, section VI). This is a difference of  $7.25 \times 10^6$  cells and approximately three orders of magnitude (compare Fig. 4a to Fig. 4b). This entire protocol was carried out three more times: (1) comparing the ancestral E(p2)–K(p1) coculture to the evolved  $E_2(p2_E)$ – $K_1(p1_K)$  coculture (Extended Data Fig. 4), (2) comparing the *E. coli* specific E(p1)–E(p2) and  $E_1(p1_E)$ – $E_2(p2_E)$  cocultures (Extended Data Fig. 5) and (3) comparing the *K. pneumoniae* specific K(p1)–K(p2) and  $K_1(p1_K)$ – $K_2(p2_K)$  cocultures (Extended Data Fig. 6). While MDR *E. coli* arose in some of the cocultures, most of all MDR cells were *K. pneumoniae*. Regardless, in each comparison, greater MDR emerged in all the cocultures that consisted of evolved pairs, supporting the predictions laid out in Fig. 2.

**Evolution generates pleiotropic effects.** In our original predictions (Fig. 2 and Extended Data Fig. 2), we assumed that mutations that compensated for the cost of the plasmid, whether plasmid-born or chromosomal, only altered fitness of the host–plasmid combination

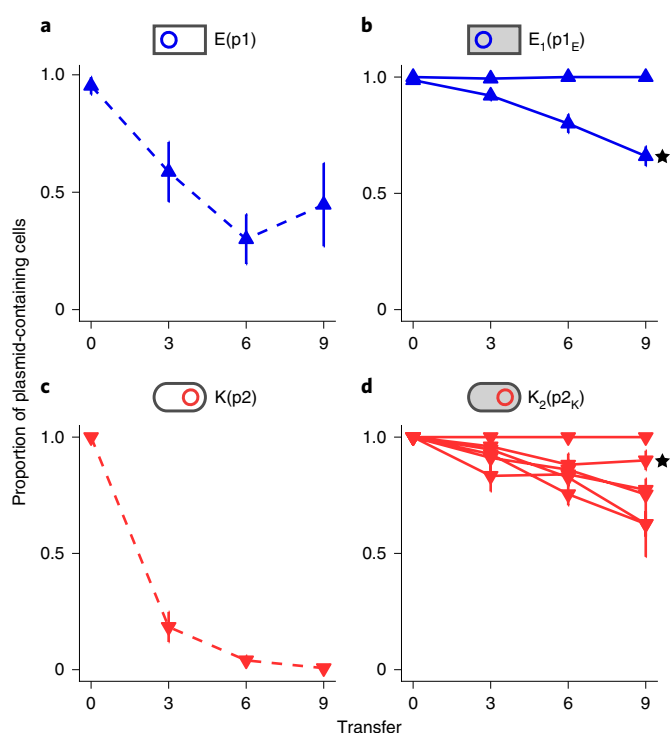


**Fig. 3 | Plasmid persistence in the absence of antibiotics increases after coevolution of plasmids with their hosts.** Dashed lines (left graphs) indicate ancestral strains. Solid lines (right graphs) indicate evolved strains. **a**, The proportion of cells containing plasmid p1 decreased rapidly in an ancestral E(p1) population in the absence of the relevant antibiotic (tetracycline). **b**, However, host–plasmid coevolution in two replicate populations with tetracycline led to greater plasmid persistence in the absence of antibiotic for both  $E_1(p1_E)$  populations. **c**, The proportion of cells containing p2 similarly decreased swiftly in an ancestral K(p2) population in the absence of the relevant antibiotic (chloramphenicol). **d**, Host–plasmid coevolution in six replicate populations with chloramphenicol resulted in greater plasmid persistence in the absence of antibiotic for all  $K_2(p2_K)$  populations. Note that for  $E_1(p1_E)$ , isolates from only two of six evolved populations were included in this assay due to inadvertent appearance of *K. pneumoniae* cells in the remaining four  $E_1(p1_E)$  populations. In these graphs, every point is the mean of the three replicate persistence assays conducted for each isolate, one from each evolved population, with upward-pointing triangles used to represent points for p1-containing populations and downward-pointing triangles used to represent points for p2-containing populations. Bars indicate the s.e.m. of replicate cultures. *E. coli* and *K. pneumoniae* icons are represented as rectangles and rods, respectively. The two star symbols denote the persistence profiles for the evolved lineages selected to be used for all further assays in this paper.

that had coevolved. However, mutant plasmids may persist longer in novel hosts<sup>34</sup> and mutant hosts may better retain novel plasmids. Indeed, Loftie-Eaton et al. showed that compensatory chromosomal mutations that increased persistence of a coevolved plasmid also enabled the same mutant host to better retain alternate plasmids, an example of pleiotropy and a phenomenon termed ‘plasmid permissiveness’<sup>14</sup>. Expanding upon our mathematical model used to support our prior predictions, we explored how this might affect the emergence of MDR in bacterial communities with multiple plasmids. Our model predicted that when compensatory mutations that generate greater plasmid persistence in one host simultaneously improve plasmid persistence in a different host, the incidence of MDR is predicted to increase (Supplementary Information, section I, and Extended Data Fig. 7).

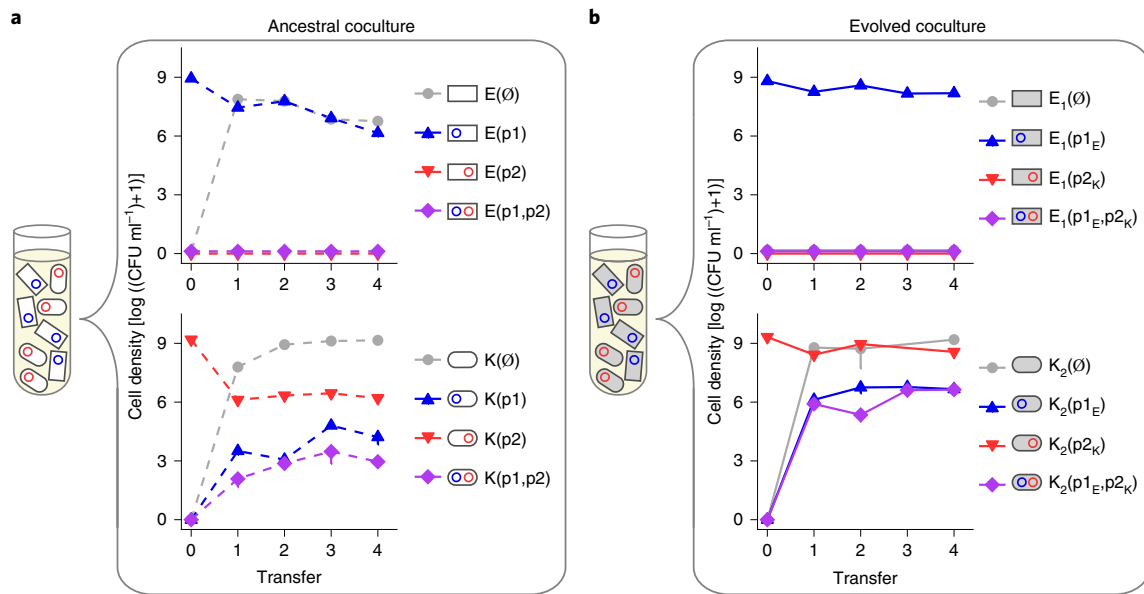


**Fig. 4 | The emergence of MDR in mixed-species cocultures increases after coevolution of plasmids with their hosts.** **a**, Three replicate cocultures of ancestral strains E(p1) and K(p2) were propagated over four transfers in the absence of antibiotics, with the initial starting coculture composition shown in the tube. Within each coculture, *E. coli* (upper graph) and *K. pneumoniae* (lower graph) were tracked via daily selective plating for each host–plasmid combination. Note that all plasmid-free, single- and double-plasmid-containing cell types become possible in either host species within the coculture due to segregational loss and conjugation. **b**, Three replicate cocultures of evolved strains E<sub>1</sub>(p1<sub>E</sub>) and K<sub>2</sub>(p2<sub>K</sub>) were propagated and tracked in an identical manner. In all plots, blue lines indicate a host containing only a p1-type plasmid (p1 or p1<sub>E</sub>); red lines indicate a host containing only a p2-type plasmid (p2 or p2<sub>K</sub>); purple lines indicate an MDR host containing both plasmid types ((p1, p2) or (p1<sub>E</sub>, p2<sub>K</sub>)); and grey lines indicate plasmid-free cells. Bars indicate the s.e.m. of three replicate cocultures. Dashed and solid lines indicate ancestral and evolved cells, respectively. The key comparison here is between the solid purple and dashed purple trajectories.

Did pleiotropy contribute to greater persistence of evolved host–plasmid pairs in our mixed-species community? Because most cells containing both plasmids in our cocultures were *K. pneumoniae*, we focused on this species. In addition to evolution increasing the persistence of the p2<sub>K</sub> plasmid in its coevolved host K<sub>2</sub> as seen in Fig. 3 (using Bayesian Information Criterion (BIC),  $\Delta\text{BIC} = -714.3$ ; Supplementary Information, section IV), persistence of p1 was higher in that same host (K<sub>2</sub>(p1)) than in the ancestral host K(p1) ( $\Delta\text{BIC} = -151.7$ ; Extended Data Fig. 8a and Supplementary Information, section VII). Thus, we see evidence of increased plasmid permissiveness: mutations in the host chromosome stabilized the coevolved plasmid p2<sub>K</sub> as well as a novel plasmid p1. Similarly, we observed increased permissiveness of *K. pneumoniae* evolved with plasmid p1 (K<sub>1</sub>) towards plasmid p2 ( $\Delta\text{BIC} = -765.7$ ; Extended Data Fig. 8b and Supplementary Information, sections V and VII). These data suggest that evolutionary changes that stabilize one particular host–plasmid relationship can have pleiotropic effects, whereby the same benefits are also experienced in novel host–plasmid combinations. These interactions can then further maintain the source pool of plasmids in the community that are available to generate more MDR cells.

**Evolution can increase MDR persistence.** In our study, the emergence of MDR is certainly facilitated by a higher likelihood of formation of cells with multiple plasmids due to the greater plasmid persistence in populations of donors and recipients containing unique plasmids. However, it may also be the case that once MDR cells are formed, they have a higher likelihood of being maintained in the population. Thus, we consider how previous host–plasmid coevolution affects the decay of plasmid-mediated antibiotic resistance in our MDR cells when selection for the plasmids is removed. In our system, this process includes transitions first from double-plasmid-containing cells to single-plasmid-containing cells and

then from single-plasmid-containing cells to plasmid-free cells (Fig. 5a). To understand this first transition we measured plasmid persistence in a population of double-plasmid-containing cells under single antibiotic exposure, which allowed the population to lose only one of the two plasmids. Specifically, in the presence of tetracycline selecting for the p1-type plasmid (p1 or p1<sub>E</sub>), we measured the persistence of the p2-type plasmid (p2 or p2<sub>K</sub>) in the ancestral host with both ancestral plasmids, K(p1, p2), as well as the evolved host with both evolved plasmids, K<sub>2</sub>(p1<sub>E</sub>, p2<sub>K</sub>) (Fig. 5b). Additionally, in the presence of chloramphenicol selecting for the p2-type plasmid, we measured the persistence of p1-type plasmid in each of the same two double-plasmid-containing hosts (Fig. 5c). Coevolution resulted in slower rates of plasmid loss in both double-plasmid-containing contexts (Fig. 5b,c;  $\Delta\text{BIC} = -19.1$  and  $-23.9$ , respectively). Turning to the transition from single-plasmid-containing cells to plasmid-free cells, we find the rate was lowered after host–plasmid coevolution (Fig. 5d,e;  $\Delta\text{BIC} = -866.0$  and  $-413.4$ , respectively; similar to that seen in Fig. 3 and Extended Data Fig. 3). However, in the flipped case where the persistence of p1<sub>K</sub> and p2<sub>E</sub> were measured in the K<sub>1</sub> host, the patterns were much muted for the transition from double-plasmid- to single-plasmid-containing cells, suggesting that host–plasmid coevolution does not always meaningfully reduce the loss rate of MDR cells (see Extended Data Fig. 9 and Supplementary Information, section VIII). In an environment with no antibiotics, MDR persistence was greater in the evolved context, K<sub>2</sub>(p1<sub>E</sub>, p2<sub>K</sub>), than in the ancestral context, K(p1, p2) ( $\Delta\text{BIC} = -2.1$ , Extended Data Fig. 10b, Supplementary Information, section VIII). In the flipped case, comparing K<sub>1</sub>(p1<sub>K</sub>, p2<sub>E</sub>) to the ancestor, MDR persistence was also greater in the evolved context, but this difference was not meaningful ( $\Delta\text{BIC} = 4.5$ , Extended Data Fig. 10a, Supplementary Information, section VIII).

Taken together, we observed that prior host–plasmid coevolution not only contributes to increased emergence of MDR in the absence



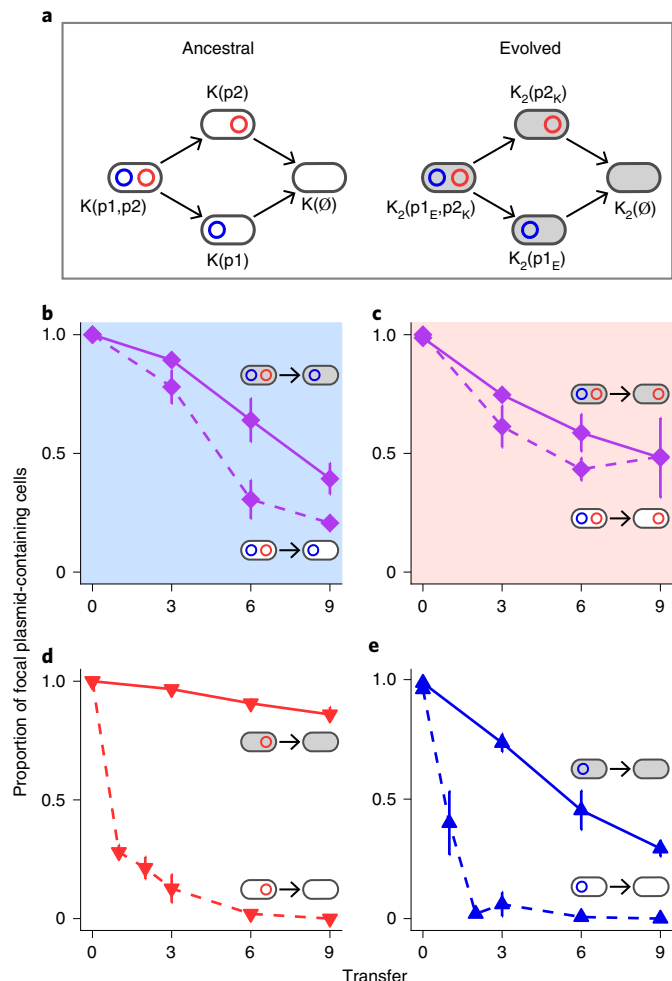


**Fig. 5 | Maintenance of antibiotic resistance and MDR increases after host-plasmid coevolution in both coevolved pairs and novel combinations of host and plasmids. a**, A lineage can lose MDR by first losing either one of the two plasmid types and then losing the remaining plasmid. Here we compare the rates of loss of a focal plasmid between ancestral and evolved strains for all single- and double-plasmid-containing cells. **b,c**, The transition from double-plasmid-containing cells to single-plasmid-containing cells. **d,e**, The transition from single-plasmid-containing cells to plasmid-free cells, with conclusions from **d** having already been drawn from a previous assay (Fig. 3). All persistence assays were done with *K. pneumoniae* as the host in an ancestral context ( $K(p_1)$ ,  $K(p_2)$  or  $K(p_1, p_2)$ ) or an evolved context ( $K_2(p_{1E})$ ,  $K_2(p_{2K})$  or  $K_2(p_{1E}, p_{2K})$ ). In all the evolved contexts,  $p_{2K}$  is the coevolved plasmid and  $p_{1E}$  is recently introduced. Furthermore, for all trajectories in **b–e**, the left cell in the displayed ‘two-cell transition icon’ possesses the focal plasmid; thus, the proportion being tracked refers to this left cell (whereas the right cell refers to a host without the focal plasmid). Persistence of the focal plasmid in a double-plasmid-containing population under selection for the alternate plasmid is higher in the evolved context than the ancestral context (**b, c**). Likewise, plasmid persistence in single-plasmid-containing populations is higher in the evolved than ancestral context (**d, e**). We also note an interesting result regarding the effect of plasmid coexistence on plasmid persistence in the ancestral strains: the dashed lines in **b** and **d** are tracking the loss of the same plasmid but in the context of the plasmid either on its own or with a coexisting plasmid (see Supplementary Information, section XI). Graph background shading indicates the presence of tetracycline (blue; selecting for  $p_1$ -type plasmid), chloramphenicol (red; selecting for  $p_2$ -type plasmid) or no antibiotics (white) during the assay. Blue, red and purple lines indicate hosts containing only the  $p_1$ -type plasmid, only the  $p_2$ -type plasmid and both plasmid types, respectively. Dashed and solid lines indicate ancestral and evolved contexts, respectively. Bars indicate s.e.m.

of antibiotics (Fig. 4) but, in some cases, can improve the maintenance of MDR (Fig. 5). This result may be particularly relevant to the practice of drug combination therapy, which is often prescribed in clinical settings to hinder the emergence of strains resistant to single antibiotics<sup>35</sup>. If MDR cells exist in a population where a drug cocktail containing the relevant antibiotics is applied, this could result in populations consisting entirely of MDR cells. Our results suggest that in some cases, these MDR cells may be maintained for a longer duration if host–plasmid coevolution has occurred.

**Discussion**

The focal plasmids  $p_1$  and  $p_2$  used in this study are broad-host-range, antibiotic resistance plasmids that were obtained from bio-solid waste that is applied on agricultural soils. Global antibiotic exposure is largely driven by agricultural practices in which antibiotics are spread on crops and given to livestock to boost food production<sup>36,37</sup>. These practices are only expected to rise<sup>38</sup> and thus concerns are also rising about the increased incidence of plasmid-mediated antibiotic resistance genes spreading from environmental isolates to the clinic. This transition is thought to be common<sup>39</sup> and is probably the cause of the recent transcontinental spread of resistance to colistin, an ‘antibiotic of last resort’<sup>40</sup> used in livestock production<sup>41</sup> and to combat clinical MDR infections. Therefore plasmids  $p_1$  and  $p_2$  are suitable for helping us better understand how novel MDR might transition from the environment to clinical settings, especially after sustained antibiotic exposure. Also relevant to our choice of plasmids is that they belong to different incompatibility (Inc) groups. This avoids any possible instability due to sharing a common replication or partitioning mechanism when the two plasmids coexist in the same cell<sup>42</sup>. We would expect the emergence of MDR cells to be muted in cases where two plasmids are from the same Inc group.

In the mixed-species cultures there is asymmetry in the emergence of MDR for *K. pneumoniae* and *E. coli*, with a much higher likelihood of MDR formation in *K. pneumoniae*. This may be largely due to poor efficiency of plasmid transfer from *K. pneumoniae* to *E. coli*, as evidenced by conjugative transfer efficiencies calculated from cell counts obtained during the first 24h of our emergence assays (Supplementary Information, section VI). Indeed, in three of the four mixed-species cocultures, conjugation from *K. pneumoniae* to *E. coli* was never observed (Supplementary Table 5). It is also possible that *K. pneumoniae* is, on average, better at maintaining multiple plasmids than is *E. coli*. This would be consistent with research suggesting that the number of plasmids per genome is higher in *K. pneumoniae* than in other Gram-negative pathogens<sup>28</sup>. Finally, it is possible that our clinically isolated *K. pneumoniae* strain is predisposed to better maintain multiple plasmids because it houses three stable native plasmids of its own (Supplementary Information, section II). However, reasoning against the last two possibilities for this particular case, plasmids  $p_1$  and  $p_2$  were originally less persistent in our *K. pneumoniae* strain than in *E. coli*, a pattern that was largely maintained across replicates after host–plasmid coevolution (compare Fig. 3 and Extended Data Fig. 3).

A list of all mutations that occurred in each evolved isolate is provided in Supplementary Information, section X. While we are unable to attribute increased persistence to any one of these mutations, interesting patterns emerged. For example, mutations in the DNA-binding transcriptional regulator of the TetR/AcrR family were found in most of the  $K_1(p_{1K})$  and  $K_2(p_{2K})$  isolates, whereas no such mutations were observed in *K. pneumoniae* hosts evolved without a plasmid ( $K_0(\emptyset)$ ; Supplementary Data 2). We note that mutations in *acrR* have been previously associated with a reduction in plasmid cost in the *E. coli* strain MG1655<sup>43</sup>, the same strain used in our study. In addition, it is interesting to consider mutations that would have multiple effects on community-level plasmid dynamics. For example, mutations in the conjugation-associated *tra* genes may

alleviate plasmid cost but also inhibit conjugation. Porse et al. found that deletions in *tra* genes on the plasmid ameliorated costs<sup>19</sup>, and in three of our six  $K_1(p1_K)$  isolates we observed large deletions of *tra* genes (Supplementary Data 2). This was not the case for the  $K_1(p1_K)$  isolate used to explore the emergence of MDR in our study but in specific cases where compensatory mutations during host–plasmid coevolution occur in *tra* genes we might expect a decrease in MDR emergence due to abolished conjugation.

Our finding that the improved persistence of two environmental drug resistance plasmids after a short period of coevolution with their new hosts resulted in emergence of novel MDR warrants future research into the consequences of enhanced coresidency of multiple plasmids inside single host cells. One side-effect may be a greater opportunity for genetic rearrangement between coresiding plasmids. Host–plasmid coevolution could thus contribute to increased generation of novel MDR *plasmids* that could then conjugate into new cells as a single transferrable unit. Lam et al. specifically voice concerns that MDR and virulence genes could easily become associated on a single plasmid in *K. pneumoniae*, due to the common co-occurrence of multiple plasmid types within that species<sup>44</sup>. Although we did not examine the MDR *K. pneumoniae* cells generated in this study for the incidence of co-integration of plasmids, this is a fruitful direction for further research as to how (and how quickly) novel MDR plasmids can originate.

Given the prevalence of antibiotic usage across the globe, we expect a wide range of bacteria to commonly experience selection for antibiotic resistance in their natural environments. Such exposure may be transient due to a defined period of drug usage or due to the migration of bacteria from environments with antibiotics to environments without drugs<sup>45</sup>. Our study and previous studies suggest this type of exposure could lead to stabilized mobile plasmids encoding antibiotic resistance. Here, we show that such coevolution can then contribute to a higher incidence of novel MDR through at least two mechanisms: by combining the resistance genes from more persistent plasmid sources in single cells at higher frequencies, and, in some cases, by limiting the rate of loss of these resistance genes from MDR cells. In this way, antibiotic usage does not only immediately select for drug resistance but simultaneously generates conditions favouring the emergence of MDR even after antibiotics are removed.

## Methods

More detailed strain descriptions and methods (including a description of our mathematical models, statistical approaches and genomic analysis) can be found in the Supplementary Information.

**Hosts and plasmids.** Bacterial hosts included strains of two Enterobacteriaceae species *E. coli* and *K. pneumoniae*: MG1655\_SR and Kp08\_R. We use the first letter of the genus name (E and K) to refer to these strains throughout. The two plasmids are conjugative, broad-host-range plasmids that were isolated from biosolids: the 61-kilobase (kb) plasmid pALTS28 (MN366357) from the plasmid group PromA, carrying genes conferring resistance to tetracycline (*tetX*), sulfonamide (*sul2*), MLS (*mph(E)* and *msr(E)*), and aminoglycosides (*aph(3')-Ib* and *aph(6)-Id*); and the 54-kb plasmid pALTS29 (MN366358) from the plasmid group IncP-1 $\beta$ , carrying genes conferring resistance to chloramphenicol (*cmIA1*), MLS (*mph(E)* and *msr(E)*), sulfonamide (*sul1*) and a gene encoding a class D beta-lactamase (*blaOXA*). We refer to these plasmids as p1 and p2 throughout. We note that both of our plasmids encode resistance to multiple drugs and thus MDR is conferred when a host contains either one. However, in this paper, we are focused on the origin of an expanded set of resistances facilitated by plasmids with distinct resistance profiles coming together in the same cell. Thus, when we discuss the emergence of MDR we are referring to the coresidency of two plasmids (each encoding resistance to distinct antibiotics) within the same cell.

**Evolution of host–plasmid pairs.** Replicate populations initiated with  $K(p1)$ ,  $K(p2)$ ,  $E(p1)$ ,  $E(p2)$ ,  $K(\emptyset)$  or  $E(\emptyset)$  were evolved in 300  $\mu$ l of Lysogeny broth (LB) in microtiter plate wells for 68 culture transfers involving a 1:60 dilution (~400 generations). Plasmid-containing strains were propagated in the presence of either 10  $\mu$ g ml<sup>-1</sup> tetracycline or 25  $\mu$ g ml<sup>-1</sup> chloramphenicol to select for p1 or p2, respectively. At the last transfer, each evolving population was diluted, plated and

a haphazardly chosen colony served as the 'evolved isolate' for the replicate lineage for subsequent assays.

**Single-plasmid persistence and permissiveness assays.** All ancestral and evolved plasmid-containing strains were inoculated under antibiotic selection for the plasmid into three replicate microtiter plate wells. Each culture was then passaged daily for nine transfers in the absence of antibiotic selection. Every three transfers, each culture was diluted and plated on LB agar to obtain single colonies. The proportion of plasmid-containing colonies out of 50 was then phenotypically determined via streaking on selective and non-selective agar. Differences between the ancestral and evolved persistence profiles were determined using a BIC model selection approach (see Supplementary Information for details). This method is in accordance with that used in previous studies measuring plasmid persistence, which is also sometimes termed 'plasmid stability'<sup>3,14,17,30,34</sup>.

**MDR emergence assay.** Plasmid-containing strains contributing to each mixture were grown in liquid cultures overnight under antibiotic selection for the appropriate plasmid. A total 1 ml of each saturated culture was spun down for 5 min at 6,000 r.p.m., the supernatant was replaced with 0.086% saline and the cells were mixed thoroughly. This was repeated three times. *K. pneumoniae* cultures were then diluted tenfold to ensure the mixed-species cultures were started with a similar number of cells per species. Both of the relevant strains were mixed in equal volumes, 5  $\mu$ l of which was used to inoculate three replicate microtiter plate wells containing 295  $\mu$ l of fresh LB. All replicates were thereafter grown in the absence of antibiotics and propagated via a 1:60 dilution every 24 h for 4 d. All possible host- and plasmid-specific cell types were tracked via selective plating daily.

**Double-plasmid persistence assays.** Double-plasmid-containing *K. pneumoniae* strains were obtained via plate matings between the recipient *K. pneumoniae* host and an *E. coli* donor. They were then tracked for the loss of each plasmid via streaking colonies onto separate antibiotic-containing plates. When the double-plasmid-containing populations were tracked for the loss of a single plasmid in the background of the alternate plasmid (the enforced presence of the non-focal plasmid), the LB growth medium was supplemented with the antibiotic concentration that inhibited the growth of any cells that did not contain the non-focal plasmid. Differences between the ancestral and evolved persistence profiles were determined using BIC model selection approaches (see Supplementary Information for details).

**Reporting Summary.** Further information on research design is available in the Nature Research Reporting Summary linked to this article.

## Data availability

All sequencing data pertaining to this project have been made available at the National Center for Biotechnology Information (SRA accession number PRJNA552385). All other data that support the findings of this study are available at <https://github.com/livkosterlitz/Figures-Jordt-et-al-2020>.

## Code availability

The StabilityToolkit package used to analyse persistence data via our plasmid population dynamic model and corresponding instructions are available at <https://github.com/jmponciano/StabilityToolkit/blob/master/RunningStabToolsPack.zip>. The code used for the nonlinear beta-binomial regression model (Supplementary Information, section IX) can be found at <https://github.com/jmponciano/JordtEtAl2020>. The code used for simulations of our mathematical model is available at [https://github.com/evokerr/Jordt\\_et\\_al\\_Gillespie\\_Code](https://github.com/evokerr/Jordt_et_al_Gillespie_Code). Code used to generate the figures can be found at <https://github.com/livkosterlitz/Figures-Jordt-et-al-2020>.

Received: 18 October 2019; Accepted: 5 March 2020;  
Published online: 6 April 2020

## References

- Norman, A., Hansen, L. H. & Sørensen, S. J. Conjugative plasmids: vessels of the communal gene pool. *Phil. Trans. R. Soc. Lond. B* **364**, 2275–2289 (2009).
- San Millan, A. & MacLean, R. C. Fitness costs of plasmids: a limit to plasmid transmission. *Microbiol. Spectr.* **5**, MTBP-0016-2017 (2017).
- Yano, H. et al. Evolved plasmid–host interactions reduce plasmid interference cost. *Mol. Microbiol.* **101**, 743–756 (2016).
- Vogwill, T. & MacLean, R. C. The genetic basis of the fitness costs of antimicrobial resistance: a meta-analysis approach. *Evol. Appl.* **8**, 284–295 (2015).
- Bergstrom, C. T., Lipsitch, M. & Levin, B. R. Natural selection, infectious transfer and the existence conditions for bacterial plasmids. *Genetics* **155**, 1505–1519 (2000).
- Harrison, E. & Brockhurst, M. A. Plasmid-mediated horizontal gene transfer is a coevolutionary process. *Trends Microbiol.* **20**, 262–267 (2012).

7. Lopatkin, A. J. et al. Persistence and reversal of plasmid-mediated antibiotic resistance. *Nat. Commun.* **8**, 1689 (2017).
8. Turner, P. E., Cooper, V. S. & Lenski, R. E. Tradeoff between horizontal and vertical modes of transmission in bacterial plasmids. *Evolution* **52**, 315 (1998).
9. Li, Y. et al. A post-segregational killing mechanism for maintaining plasmid PMF1 in its *Myxococcus fulvus* host. *Front. Cell. Infect. Microbiol.* **8**, 274 (2018).
10. Dahlberg, C. & Chao, L. Amelioration of the cost of conjugative plasmid carriage in *Escherichia coli* K12. *Genetics* **165**, 1641–1649 (2003).
11. Bouma, J. E. & Lenski, R. E. Evolution of a bacteria/plasmid association. *Nature* **335**, 351–352 (1988).
12. Starikova, I. et al. Fitness costs of various mobile genetic elements in *Enterococcus faecium* and *Enterococcus faecalis*. *J. Antimicrob. Chemother.* **68**, 2755–2765 (2013).
13. Dionisio, F., Conceição, I. C., Marques, A. C. R., Fernandes, L. & Gordo, I. The evolution of a conjugative plasmid and its ability to increase bacterial fitness. *Biol. Lett.* **1**, 250–252 (2005).
14. Loftie-Eaton, W. et al. Compensatory mutations improve general permissiveness to antibiotic resistance plasmids. *Nat. Ecol. Evol.* **1**, 1354 (2017).
15. Ridenhour, B. J. et al. Persistence of antibiotic resistance plasmids in bacterial biofilms. *Evol. Appl.* **10**, 640–647 (2017).
16. Harrison, E., Guymer, D., Spiers, A. J., Paterson, S. & Brockhurst, M. A. Parallel compensatory evolution stabilizes plasmids across the parasitism–mutualism continuum. *Curr. Biol.* **25**, 2034–2039 (2015).
17. Stalder, T. et al. Emerging patterns of plasmid–host coevolution that stabilize antibiotic resistance. *Sci. Rep.* **7**, 4853 (2017).
18. San Millan, A. et al. Positive selection and compensatory adaptation interact to stabilize non-transmissible plasmids. *Nat. Commun.* **5**, 5208 (2014).
19. Porse, A., Schønning, K., Munck, C. & Sommer, M. O. A. Survival and evolution of a large multidrug resistance plasmid in new clinical bacterial hosts. *Mol. Biol. Evol.* **33**, 2860–2873 (2016).
20. Santos-Lopez, A. et al. Compensatory evolution facilitates the acquisition of multiple plasmids in bacteria. Preprint at bioRxiv <https://doi.org/10.1101/187070> (2017).
21. Wein, T., Hülter, N. F., Mizrahi, I. & Dagan, T. Emergence of plasmid stability under non-selective conditions maintains antibiotic resistance. *Nat. Commun.* **10**, 2595 (2019).
22. Exner, M. et al. Antibiotic resistance: what is so special about multidrug-resistant Gram-negative bacteria? *GMS Hyg. Infect. Control* **12**, <https://doi.org/10.3205/dgkh000290> (2017).
23. Oliphant, C. M. & Eroschenko, K. Antibiotic resistance, part 2: Gram-negative pathogens. *J. Nurse Pract.* **11**, 79–86 (2015).
24. *Prioritization of Pathogens to Guide Discovery, Research and Development of New Antibiotics for Drug Resistant Bacterial Infections, Including Tuberculosis* (WHO, 2017); <https://go.nature.com/2Jcr0cF>
25. McGann, P. et al. *Escherichia coli* harboring *mcr-1* and *bla<sub>CTX-M</sub>* on a novel IncF plasmid: first report of *mcr-1* in the United States. *Antimicrob. Agents Chemother.* **60**, 4420–4421 (2016).
26. de Man, T. J. B. et al. Genomic analysis of a pan-resistant isolate of *Klebsiella pneumoniae*, United States 2016. *mBio* **9**, e00440–18 (2018).
27. Navon-Venezia, S., Kondratyeva, K. & Carattoli, A. *Klebsiella pneumoniae*: a major worldwide source and shuttle for antibiotic resistance. *FEMS Microbiol. Rev.* **41**, 252–275 (2017).
28. Wyres, K. L. & Holt, K. E. *Klebsiella pneumoniae* as a key trafficker of drug resistance genes from environmental to clinically important bacteria. *Curr. Opin. Microbiol.* **45**, 131–139 (2018).
29. Wyres, K. L. & Holt, K. E. *Klebsiella pneumoniae* population genomics and antimicrobial-resistant clones. *Trends Microbiol.* **24**, 944–956 (2016).
30. Sota, M. et al. Shifts in host range of a promiscuous plasmid through parallel evolution of its replication initiation protein. *ISME J.* **4**, 1568–1580 (2010).
31. Gelder, L. D. et al. Combining mathematical models and statistical methods to understand and predict the dynamics of antibiotic-sensitive mutants in a population of resistant bacteria during experimental evolution. *Genetics* **168**, 1131–1144 (2004).
32. Ponciano, J. M., Gelder, L. D., Top, E. M. & Joyce, P. The population biology of bacterial plasmids: a hidden Markov model approach. *Genetics* **176**, 957–968 (2007).
33. Loftie-Eaton, W. et al. Evolutionary paths that expand plasmid host-range: implications for spread of antibiotic resistance. *Mol. Biol. Evol.* **33**, 885–897 (2016).
34. De Gelder, L., Williams, J. J., Ponciano, J. M., Sota, M. & Top, E. M. Adaptive plasmid evolution results in host-range expansion of a broad-host-range plasmid. *Genetics* **178**, 2179–2190 (2008).
35. Tängdén, T. Combination antibiotic therapy for multidrug-resistant Gram-negative bacteria. *Ups. J. Med. Sci.* **119**, 149–153 (2014).
36. Manyi-Loh, C., Mamphweli, S., Meyer, E. & Okoh, A. Antibiotic use in agriculture and its consequential resistance in environmental sources: potential public health implications. *Molecules* **23**, 795 (2018).
37. Vaz-Moreira, I., Ferreira, C., Nunes, O. C. & Manaia, C. M. in *Antibiotic Drug Resistance* (eds Capelo-Martínez, J.-L. & Igrejas, G.) 211–238 (John Wiley & Sons, 2019).
38. Van Boeckel, T. P. et al. Global trends in antimicrobial use in food animals. *Proc. Natl Acad. Sci. USA* **112**, 5649–5654 (2015).
39. Crofts, T. S., Gasparrini, A. J. & Dantas, G. Next-generation approaches to understand and combat the antibiotic resistome. *Nat. Rev. Microbiol.* **15**, 422–434 (2017).
40. Kaye, K. S., Pogue, J. M., Tran, T. B., Nation, R. L. & Li, J. Agents of last resort: polymyxin resistance. *Infect. Dis. Clin. N. Am.* **30**, 391–414 (2016).
41. Schwarz, S. & Johnson, A. P. Transferable resistance to colistin: a new but old threat. *J. Antimicrob. Chemother.* **71**, 2066–2070 (2016).
42. Novick, R. P. Plasmid incompatibility. *Microbiol. Mol. Biol. Rev.* **51**, 381–395 (1987).
43. Bottery, M. J., Wood, A. J. & Brockhurst, M. A. Adaptive modulation of antibiotic resistance through intragenomic coevolution. *Nat. Ecol. Evol.* **1**, 1364–1369 (2017).
44. Lam, M. M. C. et al. Convergence of virulence and MDR in a single plasmid vector in MDR *Klebsiella pneumoniae* ST15. *J. Antimicrob. Chemother.* **74**, 1218–1222 (2019).
45. Harrison, E., Hall, J. P. J. & Brockhurst, M. A. Migration promotes plasmid stability under spatially heterogeneous positive selection. *Proc. R. Soc. B* **285**, 20180324 (2018).

## Acknowledgements

This work is supported by the National Institute of Allergy and Infectious Diseases Extramural Activities grant no. R01 A1084918 of the National Institutes of Health and through the National Science Foundation (NSF) under Cooperative Agreement no. DBI-0939454. H.J. was supported in part by Public Health Service, National Research Service Award grant no. T32GM007270, from the National Institute of General Medical Sciences. O.K. was supported in part by the NSF Graduate Research Fellowship grant no. DGE-1762114. B.K. was supported in part by the NSF Career Award grant no. DEB-0952825. We thank W. Loftie-Eaton for aiding in initial training of experimental techniques and the Kerr and Top laboratories for useful suggestions on the manuscript.

## Author contributions

H.J., B.K. and E.M.T. designed the study. H.J. performed experiments. O.K. facilitated part of the experiments. H.J., B.K. and J.M.P. performed the statistical analyses. T.S. processed samples for sequencing. T.S. and O.K. performed the genomic analyses. B.K. developed the mathematical models. H.J., B.K., E.M.T., O.K., T.S. and J.M.P. wrote the manuscript.

## Competing interests

The authors declare no competing interests.

## Additional information

Extended data is available for this paper at <https://doi.org/10.1038/s41559-020-1170-1>.

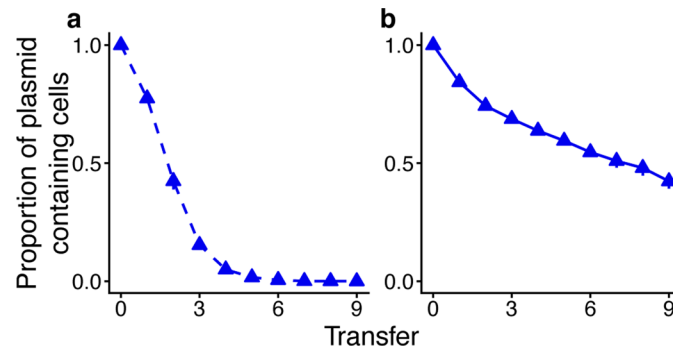
Supplementary information is available for this paper at <https://doi.org/10.1038/s41559-020-1170-1>.

Correspondence and requests for materials should be addressed to E.M.T. or B.K.

Reprints and permissions information is available at [www.nature.com/reprints](http://www.nature.com/reprints).

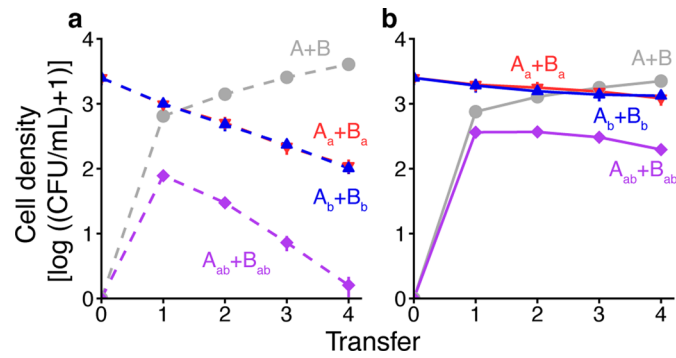
Publisher's note Springer Nature remains neutral with regard to jurisdictional claims in published maps and institutional affiliations.

© The Author(s), under exclusive licence to Springer Nature Limited 2020

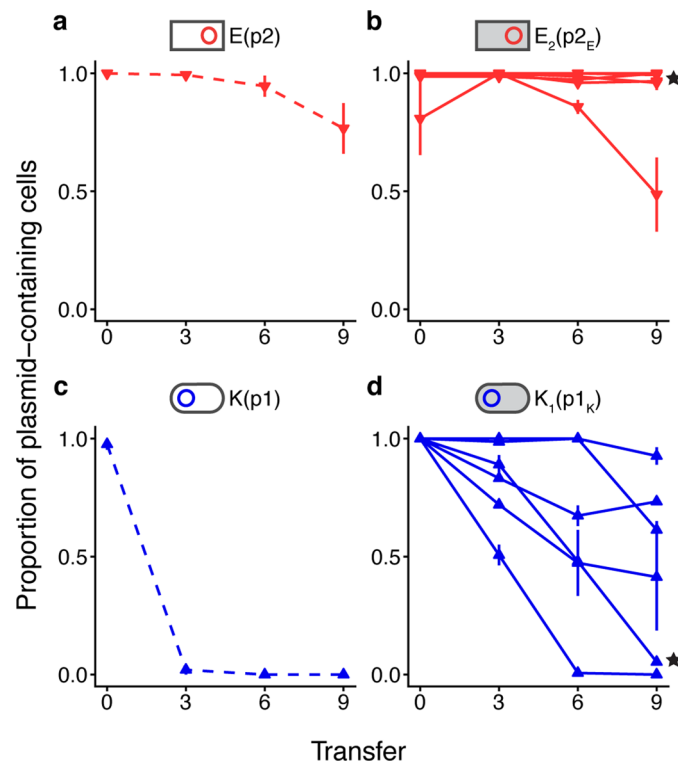


**Extended Data Fig. 1 | Model simulation of plasmid persistence.** **a**, The Gillespie algorithm was used to simulate population dynamics with  $\mu^*=0.7$ ,  $c=0.2$ ,  $K_R=0.004$ ,  $\lambda=0.05$ ,  $\tau=0.00001$ , and  $1/\psi=0.000002$ , and the dynamic variables were initialized with  $R_0=0.02$ ,  $A_0=0$ , and  $A_{s,0}=200$ . Many of the parameter values used here are similar to those from a previous parameterized model<sup>2</sup>. The average plasmid-bearing proportion of the simulated population over 10 replicates is shown as points, with each point located at the time closest to the end of the relevant 8-hour transfer period, after which a 60-fold dilution and resource replenishment occurred. The dashed line indicates that ancestral populations are being tracked. **b**, Evolution is integrated by a reduction in the cost of plasmid carriage. Here we set  $p=0.99$ , which makes the effective cost of the plasmid two orders of magnitude lower. Consequently, the loss of the plasmid from the evolved population is slower compared to its ancestor in part a. The solid line indicates that evolved populations are being tracked.

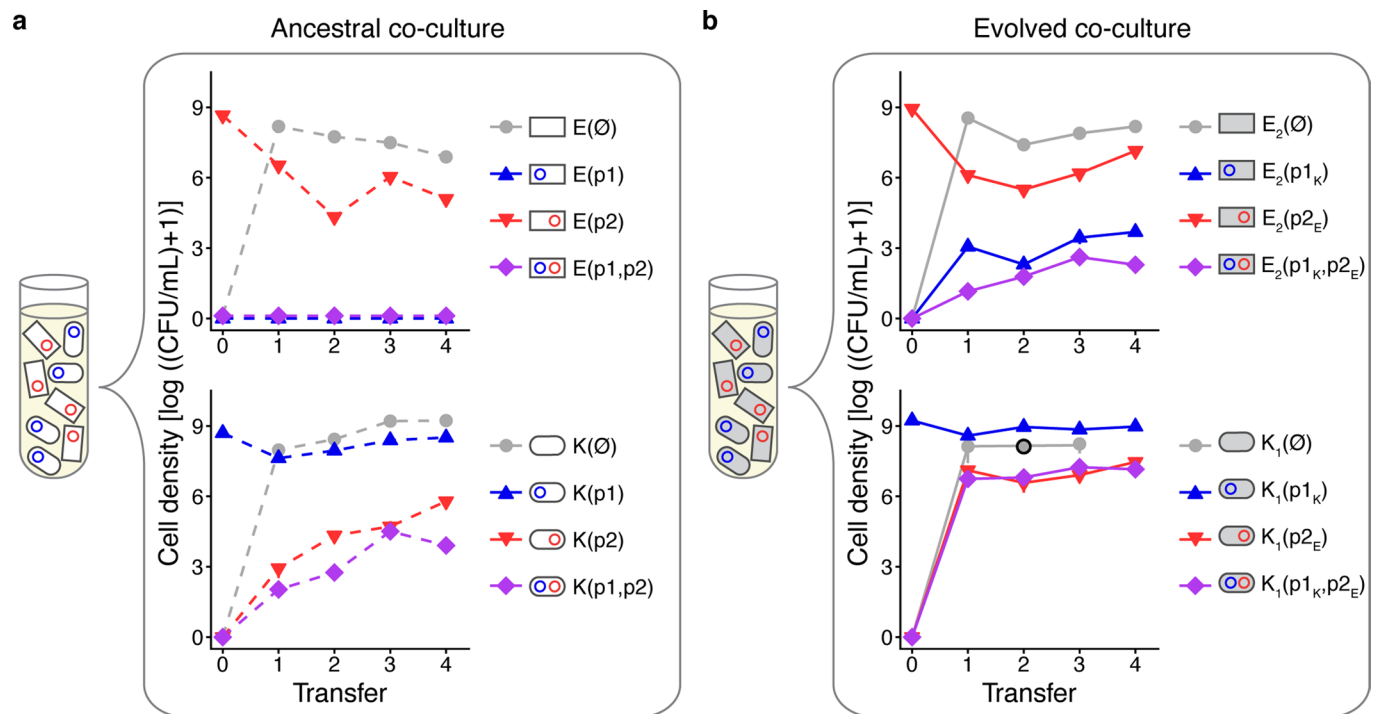




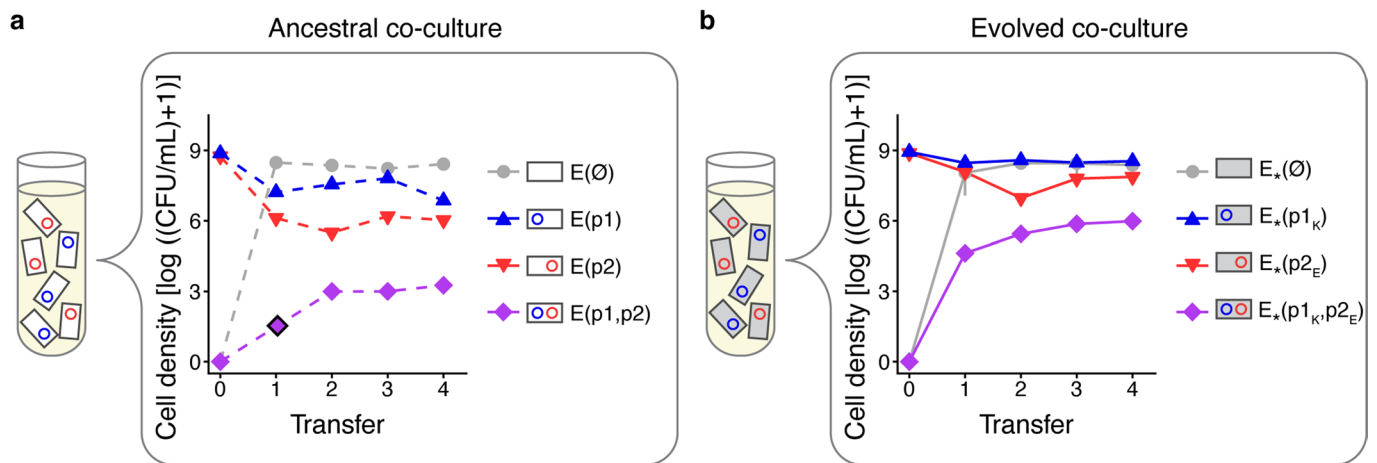
**Extended Data Fig. 2 | Model simulation of MDR emergence. a**, The Gillespie algorithm was used to simulate community dynamics with parameters as in Extended Data Fig. 1, and initial non-zero variables set to  $A_{a,0}=200$ ,  $B_{b,0}=200$ , and  $R_0=0.02$ . The average cell densities for the simulated population over 10 replicates are shown as points, with each point located at the time closest to the end of the relevant transfer period. The dashed lines indicate that ancestral populations are being tracked. **b**, Evolution is incorporated by a reduction in the plasmid cost ( $\rho=0.99$ ) for both plasmids in their native hosts. Consequently, the density of MDR cells is higher compared to the ancestral community in part a. The solid lines indicate that evolved populations are being tracked.



**Extended Data Fig. 3 | Plasmid persistence in the absence of antibiotics increases after coevolution of plasmids with their hosts.** Dashed lines (left graphs) indicate ancestral strains. Solid lines (right graphs) indicate evolved strains. **a**, The proportion of cells containing plasmid p2 decreased in an ancestral  $E(p_2)$  population in the absence of the relevant antibiotic (chloramphenicol). However, coevolution of this host and plasmid in six replicate populations with chloramphenicol led to **(b)** greater plasmid persistence in the absence of antibiotic for nearly all of the  $E_2(p_{2E})$  populations. **c**, The proportion of cells containing p1 rapidly decreased in an ancestral  $K(p_1)$  population in the absence of the relevant antibiotic (tetracycline). Host-plasmid coevolution in six replicate populations with tetracycline resulted in **(d)** greater plasmid persistence in the absence of antibiotic for all  $K_1(p_{1K})$  populations. In these graphs, every point is the mean of the three replicate persistence assays conducted for each isolate, with upward-pointing triangles used to represent points for p1-containing populations, and downward-pointing triangles used to represent points for p2-containing populations. Bars indicate the s.e.m. of replicate cultures. *E. coli* and *K. pneumoniae* icons are represented as rectangles and rods, respectively. The two “★” symbols denote the persistence profiles for the evolved strains selected to be used for all further assays.

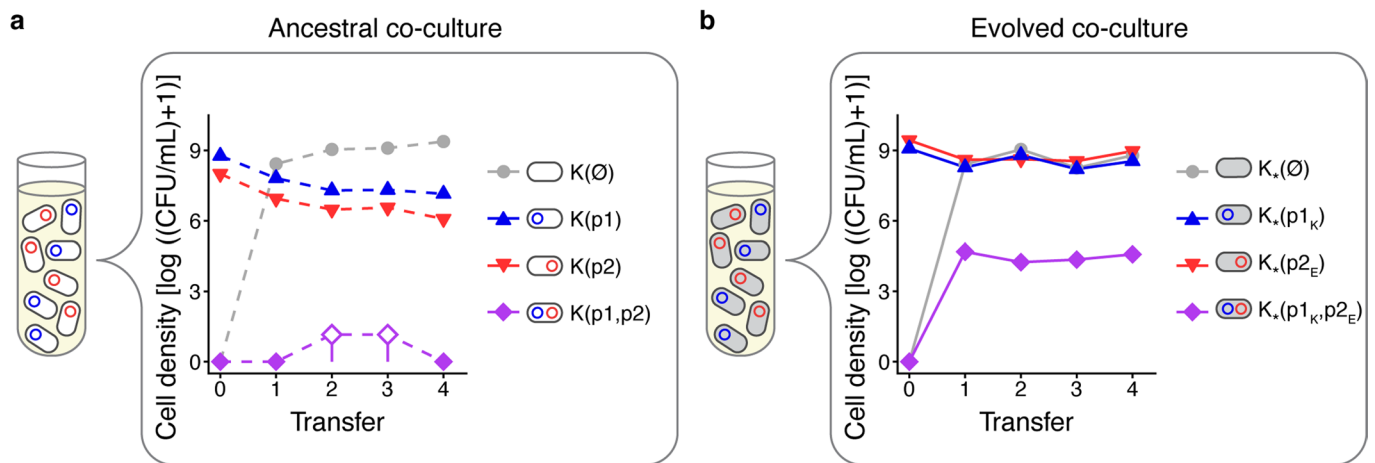


**Extended Data Fig. 4 | The emergence of MDR in mixed-species cocultures increases after coevolution of plasmids with their hosts.** **a**, Three replicate cocultures of ancestral strains  $E(p2)$  and  $K(p1)$  were propagated over 4 transfers in the absence of antibiotics. Within each coculture, *E. coli* (upper graph) and *K. pneumoniae* (lower graph) were tracked via daily selective plating for each host-plasmid combination. **b**, Three replicate cocultures of evolved strains  $E_2(p2_E)$  and  $K_1(p1_K)$  were propagated and tracked in an identical manner. In all plots, blue lines indicate a host containing only a p1-type plasmid (p1 or  $p1_K$ ); red lines indicate a host containing only a p2-type plasmid (p2 or  $p2_E$ ); purple lines indicate an MDR host containing both plasmid types ((p1, p2) or ( $p1_K$ ,  $p2_E$ )); and grey lines indicate plasmid-free cells. Bars indicate the s.e.m. of three replicate cocultures. Dashed and solid lines indicate ancestral and evolved cells, respectively. Note that the point outlined in black in the plasmid-free cell trajectory indicates that the point was interpolated using the previous and following points on the trajectory, due to missing data (see Supplementary Information VI, section a). The key comparison here is between the solid purple and dashed purple trajectories. Cumulatively, there are significantly more MDR *K. pneumoniae* in evolved than ancestral cocultures ( $t = -19.565$ , 95% CI =  $[-44541787, -28484560]$ ,  $df = 2$ ,  $P = 0.0026$ ), by a difference of  $3.65 \times 10^7$  cells. MDR *E. coli* exhibits a similar trend, although the mean difference of  $5.83 \times 10^2$  cells is not significant ( $t = -2.6576$ , 95% CI =  $[-1527.7, 361.1]$ ,  $df = 2$ ,  $P = 0.1172$ ).

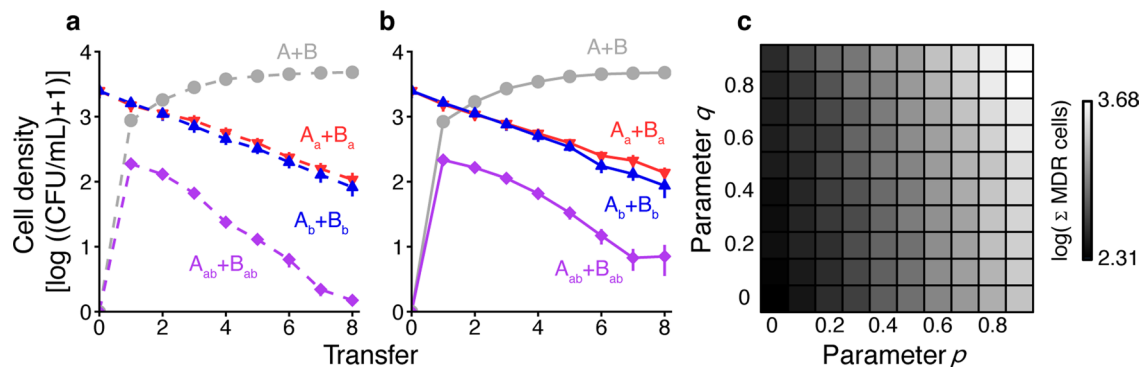


**Extended Data Fig. 5 | The emergence of MDR in *E. coli* cocultures increases after coevolution of plasmids with their hosts.** **a**, Three replicate cocultures of ancestral strains  $E(p_1)$  and  $E(p_2)$  were propagated over 4 transfers in the absence of antibiotics. Within each coculture, *E. coli* cells were tracked via daily selective plating for each host–plasmid combination. **b**, Three replicate cocultures of evolved strains  $E_1(p_{1\kappa})$  and  $E_2(p_{2\epsilon})$  were propagated and tracked in an identical manner. The asterisk notation ( $E_*$ ) indicates either host  $E_1$  or  $E_2$ . In all plots, blue lines indicate a host containing only a p1-type plasmid ( $p_1$  or  $p_{1\kappa}$ ); red lines indicate a host containing only a p2-type plasmid ( $p_2$  or  $p_{2\epsilon}$ ); purple lines indicate an MDR host containing both plasmid types ( $(p_1, p_2)$  or  $(p_{1\kappa}, p_{2\epsilon})$ ); and grey lines indicate plasmid-free cells. Bars indicate the s.e.m. of three replicate cocultures. Dashed and solid lines indicate ancestral and evolved cells, respectively. Note that the point outlined in black in the double-plasmid-containing cell trajectory indicates that the point was interpolated using the previous and following points on the trajectory, due to missing data (see Supplementary Information VI, section a). The key comparison here is between the solid purple and dashed purple trajectories. Cumulatively there are significantly more MDR *E. coli* in evolved than ancestral cocultures by a difference of  $1.53 \times 10^6$  cells ( $t = -27.465$ , 95% CI =  $[-1767743, -1288990]$ ,  $df = 2.0005$ ,  $P = 0.001321$ ).

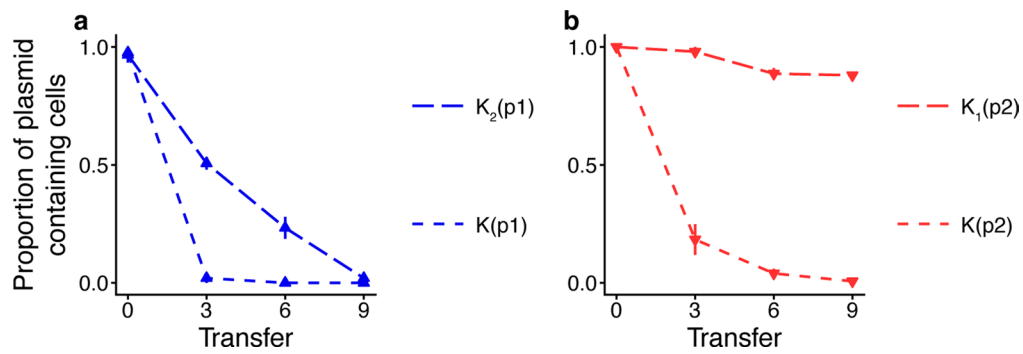




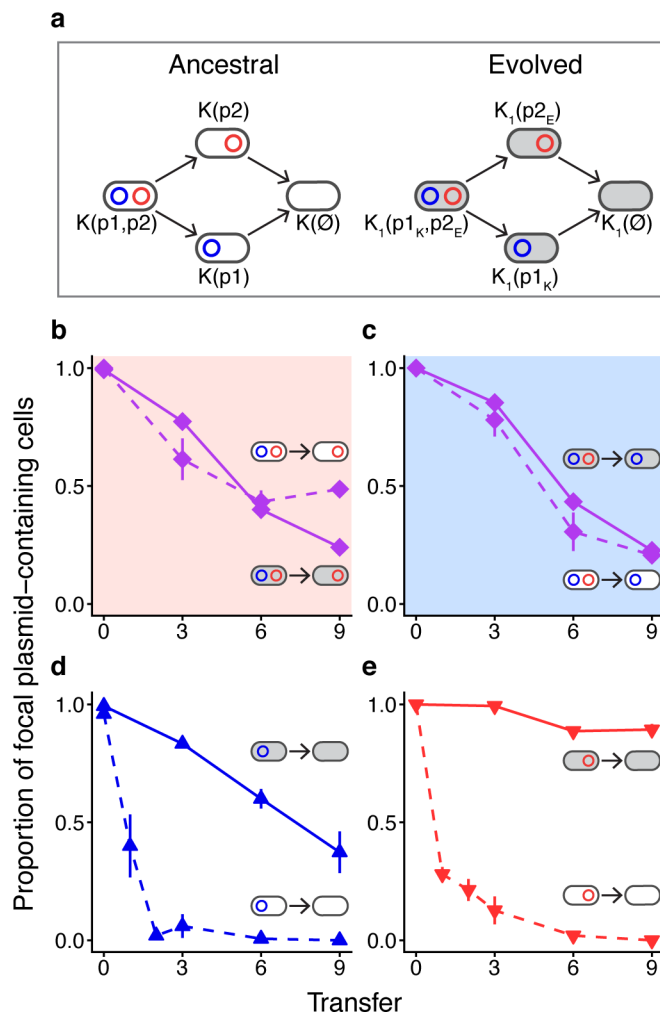
**Extended Data Fig. 6 | The emergence of MDR in *K. pneumoniae* cocultures increases after coevolution of plasmids with their hosts.** **a**, Three replicate cocultures of ancestral strains  $K(p_1)$  and  $K(p_2)$  were propagated over 4 transfers in the absence of antibiotics. Within each coculture, *K. pneumoniae* cells were tracked via daily selective plating for each host–plasmid combination. **b**, Three replicate cocultures of evolved strains  $K_1(p_{1_K})$  and  $K_2(p_{2_E})$  were propagated and tracked in an identical manner. The asterisk notation ( $K_*$ ) indicates either host  $K_1$  or  $K_2$ . In all plots, blue lines indicate a host containing only a  $p_1$ -type plasmid ( $p_1$  or  $p_{1_K}$ ); red lines indicate a host containing only a  $p_2$ -type plasmid ( $p_2$  or  $p_{2_E}$ ); purple lines indicate an MDR host containing both plasmid types ( $(p_1, p_2)$  or  $(p_{1_K}, p_{2_E})$ ); and grey lines indicate plasmid-free cells. Bars indicate the s.e.m. of three replicate cocultures. Dashed and solid lines indicate ancestral and evolved cells, respectively. Note that the open diamonds in the ancestral double-plasmid-containing cell trajectories indicate that the colony counts fell below our false positive threshold (see Supplementary Information VI, section a). The key comparison here is between the solid purple and dashed purple trajectories. Cumulatively there are significantly more MDR *K. pneumoniae* in evolved than ancestral cocultures by a difference of  $1.08 \times 10^5$  cells ( $t = -7.174$ , 95% CI =  $[-172891.2, -43255.5]$ ,  $df = 2$ ,  $P = 0.01888$ ).



**Extended Data Fig. 7 | Model simulation of MDR emergence with pleiotropic effects. a**, The Gillespie algorithm was used to simulate community dynamics with parameters and initial variable settings as in Extended Data Figs. 1 and 2. The average cell densities for the simulated population over 10 replicates are shown as points, with each point located at the time closest to the end of the relevant transfer period. Here we assume that evolutionary changes have led to a reduction in the plasmid cost ( $p=0.5$ ) for both plasmids in their native hosts, but note for any non-native configuration there is no cost reduction ( $q=0$ ). **b**, Here we allow for pleiotropic effects—namely a reduction of plasmid cost in non-native configurations ( $q=0.5$ ). Although the difference is not substantial, the density of MDR cells is greater at every transfer. **c**, More generally, we show a (literal) density plot for different  $p$ - $q$  combinations. The grey level for each square is the log of the cumulative density of MDR cells at the end of 8 transfers for each combination of direct ( $p$ ) and pleiotropic ( $q$ ) effects of compensatory mutations. Greater reductions of plasmid costs in either native or non-native contexts correspond to higher incidence of MDR.

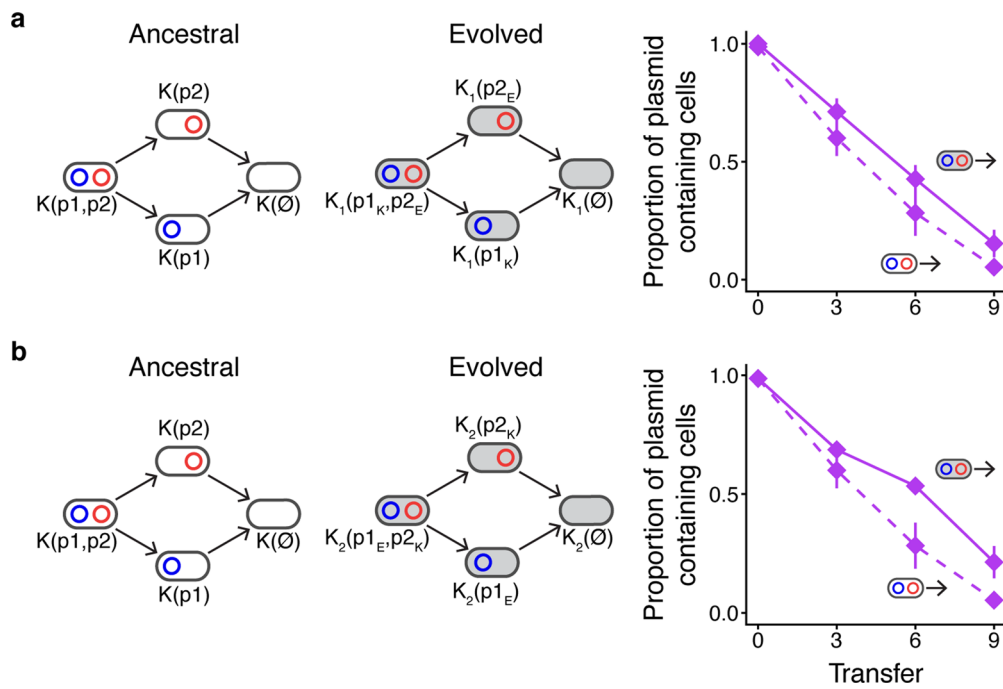


**Extended Data Fig. 8 | Hosts evolved with one plasmid became more permissive towards a novel plasmid.** Longer dashed lines indicate a host that was coevolved with the alternate plasmid. Shorter dashed lines represent ancestral host–plasmid pairs and are identical to those seen in Fig. 3 and Extended Data Fig. 3. **a**, Persistence of the ancestral plasmid p1 was greater in  $K_2(p1)$  than it was in  $K(p1)$  ( $\Delta\text{BIC} = -151.7$ ), indicating that changes in the host due to evolution with alternate plasmid type p2 have allowed it to better retain novel plasmid p1 (that is, permissiveness is observed). **b**, Persistence of the ancestral plasmid p2 was greater in  $K_1(p2)$  than it was in  $K(p2)$  ( $\Delta\text{BIC} = -765.7$ ), again indicating permissiveness. Each point is the mean of three replicate persistence assays. Bars indicate the s.e.m.



**Extended Data Fig. 9 | The dynamics of antibiotic resistance and MDR persistence after host-plasmid coevolution, in both coevolved pairs and novel combinations of host and plasmids.** **a**, A lineage can lose MDR by first losing either one of the two plasmid types and then losing the remaining plasmid. Here we compare the rates of loss of a focal plasmid between ancestral and evolved strains for all single- and double-plasmid-containing cells. **b**, and **c**, represent the transition from double-plasmid-containing cells to single-plasmid-containing cells, whereas **d**, and **e**, show the transition from single-plasmid-containing cells to plasmid-free cells, with conclusions from **(d)** having already been drawn from a previous assay (Extended Data Fig. 3c, d). All persistence assays were done with *K. pneumoniae* as the host in an ancestral context ( $K(p_1)$ ,  $K(p_2)$  or  $K(p_1, p_2)$ ) or an evolved context ( $K_1(p_{1_K})$ ,  $K_1(p_{2_E})$  or  $K_1(p_{1_K}, p_{2_E})$ ). In all the evolved contexts,  $p_{1_K}$  is the coevolved plasmid and  $p_{2_E}$  is recently introduced. Furthermore, for all trajectories in panels **(b)–(e)**, the left cell in the displayed “two-cell transition icon” possesses the focal plasmid; thus, the proportion being tracked refers to this left cell (whereas the right cell refers to a host *without* the focal plasmid). **(b)**, Persistence of the focal plasmid in a double-plasmid-containing population under selection for the alternate plasmid is initially higher and ultimately different in the evolved context compared to the ancestral context for the  $p_1$ -type plasmid ( $\Delta\text{BIC} = -27.7$ , Supplementary Table 7) and **(c)**, higher but not meaningfully different compared to the ancestral context for the  $p_2$ -type plasmid ( $\Delta\text{BIC} = 11.7$ , Supplementary Table 7). **(d)**, Plasmid persistence in a single-plasmid-containing population is higher in the evolved context than the ancestral context for the  $p_1$ -type plasmid ( $\Delta\text{BIC} = -552.3$ , Supplementary Table 7) and **(e)**  $p_2$ -type plasmid ( $\Delta\text{BIC} = -893.7$ , Supplementary Table 7). We also note an interesting result regarding the effect of plasmid coresidency on plasmid persistence in the ancestral strains: the dashed lines in **(b)** and **(d)** are tracking the loss of the same plasmid but in the context of the plasmid either on its own or with a coresiding plasmid (see Supplementary Information XI). Graph background shading and line colours are identical to Fig. 5. Dashed and solid lines indicate ancestral and evolved contexts, respectively. Bars indicate s.e.m.





**Extended Data Fig. 10 | The dynamics of MDR persistence in the absence of antibiotics. a**, A *K. pneumoniae* cell lineage loses MDR by first losing either one of the two plasmid types and then losing whatever plasmid type remains. The diagrams in this figure are repeated from Fig. 5a and Extended Data Fig. 9a. Here we compare the rates of plasmid loss between ancestral and evolved strains for all double-plasmid-containing cells as their lineages transition to further plasmid loss. White cell backgrounds indicate ancestral hosts and plasmids. Grey cell backgrounds indicate evolved hosts and plasmids. Plasmid persistence is measured as the transition from double-plasmid-containing cells to either single-plasmid-containing cells or plasmid-free cells. Plasmid persistence assays were done with *K. pneumoniae* as the host in an ancestral context ( $K(p_1, p_2)$ ; dashed line) or in an evolved context ( $K_1(p_1_K, p_2_E)$ ; solid line). While there appears to be greater MDR persistence in the evolved context, there is no meaningful difference between the two persistence curves ( $\Delta\text{BIC} = 4.5$ ) according to a nonlinear Beta-binomial regression model (see Supplementary Information IX). **b**, We compare the same ancestral persistence curve (dashed line) to the alternate evolved context ( $K_2(p_1_E, p_2_K)$ ; solid line), in which case there is a meaningful difference between the curves ( $\Delta\text{BIC} = -2.1$ ; Supplementary Information IX). No antibiotics were present during the assay. Purple lines indicate MDR hosts containing both plasmid types. Bars indicate s.e.m.

## Reporting Summary

Nature Research wishes to improve the reproducibility of the work that we publish. This form provides structure for consistency and transparency in reporting. For further information on Nature Research policies, see [Authors & Referees](#) and the [Editorial Policy Checklist](#).

### Statistics

For all statistical analyses, confirm that the following items are present in the figure legend, table legend, main text, or Methods section.

n/a Confirmed

- The exact sample size ( $n$ ) for each experimental group/condition, given as a discrete number and unit of measurement
- A statement on whether measurements were taken from distinct samples or whether the same sample was measured repeatedly
- The statistical test(s) used AND whether they are one- or two-sided  
*Only common tests should be described solely by name; describe more complex techniques in the Methods section.*
- A description of all covariates tested
- A description of any assumptions or corrections, such as tests of normality and adjustment for multiple comparisons
- A full description of the statistical parameters including central tendency (e.g. means) or other basic estimates (e.g. regression coefficient) AND variation (e.g. standard deviation) or associated estimates of uncertainty (e.g. confidence intervals)
- For null hypothesis testing, the test statistic (e.g.  $F$ ,  $t$ ,  $r$ ) with confidence intervals, effect sizes, degrees of freedom and  $P$  value noted  
*Give  $P$  values as exact values whenever suitable.*
- For Bayesian analysis, information on the choice of priors and Markov chain Monte Carlo settings
- For hierarchical and complex designs, identification of the appropriate level for tests and full reporting of outcomes
- Estimates of effect sizes (e.g. Cohen's  $d$ , Pearson's  $r$ ), indicating how they were calculated

*Our web collection on [statistics for biologists](#) contains articles on many of the points above.*

### Software and code

Policy information about [availability of computer code](#)

Data collection

The code used to generate the data from our mathematical model is available at [https://github.com/evokerr/Jordt\\_et\\_al\\_Gillespe\\_Code](https://github.com/evokerr/Jordt_et_al_Gillespe_Code)

Data analysis

The StabilityToolkit package used to analyze persistence data via our plasmid population dynamic model and corresponding instructions are available at <https://github.com/jmponciano/StabilityToolkit/blob/master/RunningStabToolsPack.zip>. The code used for the non-linear Beta-binomial regression model (Supplemental Materials IX) can be found at <https://github.com/jmponciano/JordtEtAl2020>. Code used to generate all figures can be found at <https://github.com/livkosterlitz/Figures-Jordt-et-al-2020>.

For manuscripts utilizing custom algorithms or software that are central to the research but not yet described in published literature, software must be made available to editors/reviewers. We strongly encourage code deposition in a community repository (e.g. GitHub). See the Nature Research [guidelines for submitting code & software](#) for further information.

### Data

Policy information about [availability of data](#)

All manuscripts must include a [data availability statement](#). This statement should provide the following information, where applicable:

- Accession codes, unique identifiers, or web links for publicly available datasets
- A list of figures that have associated raw data
- A description of any restrictions on data availability

All sequencing data pertaining to this project have been made available at the National Center for Biotechnology Information (SRA accession number PRJNA552385). All other data that support the findings of this study are available from the corresponding authors upon request.

## Field-specific reporting

Please select the one below that is the best fit for your research. If you are not sure, read the appropriate sections before making your selection.

- Life sciences       Behavioural & social sciences       Ecological, evolutionary & environmental sciences

For a reference copy of the document with all sections, see [nature.com/documents/nr-reporting-summary-flat.pdf](https://www.nature.com/documents/nr-reporting-summary-flat.pdf)

## Life sciences study design

All studies must disclose on these points even when the disclosure is negative.

Sample size	The number of replicates (n = 3 for all experiments) was chosen based on the scale of the project and consistency with other similar published studies. Our results demonstrate that the selected sample sizes were sufficient to detect significant differences in most of our comparisons.
Data exclusions	No data were excluded from analyses.
Replication	Our entire experiment was repeated three times with different host-plasmid combinations. Our findings were largely consistent across these different experimental runs, suggesting a degree of robustness to our conclusions.
Randomization	All clonal populations in this study were initiated from colonies selected haphazardly. All experiments and assays were conducted in well-controlled and condition-uniform environments.
Blinding	The investigator was not blinded during data collection as the measured variables for the assays were dichotomous and not subjective.

## Reporting for specific materials, systems and methods

We require information from authors about some types of materials, experimental systems and methods used in many studies. Here, indicate whether each material, system or method listed is relevant to your study. If you are not sure if a list item applies to your research, read the appropriate section before selecting a response.

### Materials & experimental systems

n/a	Involvement in the study
<input checked="" type="checkbox"/>	<input type="checkbox"/> Antibodies
<input checked="" type="checkbox"/>	<input type="checkbox"/> Eukaryotic cell lines
<input checked="" type="checkbox"/>	<input type="checkbox"/> Palaeontology
<input checked="" type="checkbox"/>	<input type="checkbox"/> Animals and other organisms
<input checked="" type="checkbox"/>	<input type="checkbox"/> Human research participants
<input checked="" type="checkbox"/>	<input type="checkbox"/> Clinical data

### Methods

n/a	Involvement in the study
<input checked="" type="checkbox"/>	<input type="checkbox"/> ChIP-seq
<input checked="" type="checkbox"/>	<input type="checkbox"/> Flow cytometry
<input checked="" type="checkbox"/>	<input type="checkbox"/> MRI-based neuroimaging